Supplemental Material

Global mortality from outdoor fine particle pollution generated by fossil fuel combustion: Results from GEOS-Chem

Karn Vohra[1*], Alina Vodonos[2], Joel Schwartz[2], Eloise A. Marais[3,a], Melissa P. Sulprizio[4], Loretta J. Mickley[4]

[1] School of Geography, Earth and Environmental Sciences, University of Birmingham, Birmingham, UK

[2] Harvard T.H. Chan School of Public Health, Department of Environmental Health, Harvard University, Boston, MA, USA

[3] Department of Physics and Astronomy, University of Leicester, Leicester, UK

[4] John A. Paulson School of Engineering and Applied Sciences, Harvard University, Cambridge, MA, USA

[a] Now at: Department of Geography, University College London, London, UK

* Corresponding author: Karn Vohra, Phone: +44 7716496867,

Email: kxv745@student.bham.ac.uk

$PM_{2.5}$ mortality concentration –response model

Figure S5. Estimates for long-term $PM_{2.5}$ mortality dose-response, drawn from the meta-analysis of long-term association between $PM_{2.5}$ and mortality.

Figure S6. Hazard Ratio based on GEMM function (Burnett et al., 2018) compared to the Hazard Ration based on the meta-analysis.

Table S2. Extended data. Global regions, number of deaths, attributable fraction (%) for the population above 14 years old attributable to fine particulate matter ($PM_{2.5}$) exposure.

References

Description of GEOS-Chem.

GEOS-Chem is a three-dimensional chemical transport model that includes detailed oxidant-aerosol chemistry in the troposphere and is used by more than 80 groups worldwide (www.geos-chem.org). The model is widely cited in the peer-reviewed literature – e.g., more than 4000 times in the year 2017 alone (http://acmg.seas.harvard.edu/geos/geos_pub.html). The model has been frequently applied to interpret observed $PM_{2.5}$ in regions dominated by anthropogenic sources – e.g., China (Aunan et al., 2018), Korea (Lee et al., 2017), India (Venkataraman et al., 2018), and the US (Di et al., 2016; Silvern et al., 2017); and validation has been performed for specific source sectors – e.g., transportation (Travis et al., 2016), biogenic sources (Marais et al., 2017), and power plants (S. W. Wang et al., 2012). Here we use GEOS-Chem v10-01, driven by 2012 GEOS-5 meteorology (gmao.gsfc.nasa.gov/GEOS_systems/). The GEOS-5 data are produced at 0.5°×0.667° horizontal resolution and are re-gridded here to 2°×2.5° for the global simulation. We also perform four regional simulations – for Europe, North America, Africa, and Asia – and for these simulations we keep the native grid resolution. Boundary conditions at 2°×2.5° from the global simulation are applied to these regional simulations. Most fine-scale, regional models, such as the Community Multiscale Air Quality Model, rely on chemical boundary conditions from global models with different chemical schemes, but our approach permits application of a consistent scheme across the globe. The 0.5°×0.667° horizontal resolution in GEOS-Chem over key regions is, however, relatively coarse compared to that in some other regional models. Y. Li et al. (2016) show that application of coarse resolution leads

to an underestimate of health impacts of 8%, implying that our mortality estimates are conservative. Our choice of 2012 as the simulation year is discussed below.

GEOS-Chem simulates the mass concentrations of key particle types including sulfate, nitrate, and ammonium (Park et al., 2004; L. Zhang et al., 2012), organic carbon (Heald et al., 2006; 2011) black carbon (Q. Q. Wang et al., 2014), dust (Fairlie et al., 2007), and sea salt (Jaegle et al., 2011). Particle chemistry is coupled to gas-phase chemistry as described by (Mao et al., 2013). Gas/particle partitioning of sulfate, nitrate and ammonium (SNA) particles is computed with the ISORROPIA II thermodynamic module (Fountoukis and Nenes, 2007; Pye et al., 2009). Wet and dry deposition of particles follow Liu et al. (2001) and L. M. Zhang et al. (2001), respectively.

Emissions in GEOS-Chem are computed by the Harvard-NASA Emission Component (HEMCO) (Keller et al., 2014), which combines and regrids ensembles of user-selected emission inventories. We apply global anthropogenic emissions but supersede these with regional emissions where the latter are more reliable (Table 1). Fossil fuel emissions in Africa include (1) industry and power plants from the global inventories and (2) diffuse and inefficient combustion sources (diesel and petrol generators, ad-hoc oil refining, gas flares, kerosene use, cars, and motorcycles) from the DICE-Africa inventory (Marais and Wiedinmyer, 2016). We scale all anthropogenic inventories to 2012, as described by van Donkelaar et al. (2008). Biogenic emissions are from MEGAN v2.1 for volatile organic compounds (Guenther et al., 2012) and from Hudman et al. (2012) for soil nitrogen oxides. Lightning emissions of nitrogen oxides are computed as a function of cloud top height as described by Murray et al. (2012). Dust entrainment and deposition follow the DEAD scheme of Zender et al. (2003) as implemented in GEOS-Chem by Fairlie et al. (2007). Biomass burning emissions are from the Global Fire Emissions Database version 4 (GFED4) (Giglio et al., 2013).

For this study, we first calculate the surface fine particle mass concentrations ($PM_{2.5}$), with all emissions sources turned on. For consistency with the $PM_{2.5}$ measurement protocol set by the U.S. Environmental

Protection Agency, we assume 35% relative humidity everywhere (except for Europe) and standard ambient conditions, with temperature of 298.15 K and surface pressure of 1013.25 hPa. In Europe, we assume 50% relative humidity, as is the protocol there. We then perform the identical simulation with emissions arising from fossil fuel combustion turned off. The same meteorological fields are applied for both simulations – i.e., the simulation does not allow feedbacks from particles onto meteorology. In the no-fossil-fuel case, all fossil fuel sources are turned off in both the nested simulations and in the global simulation providing boundary conditions. The difference between the two simulations (with and without fossil fuel) represents the contribution of fossil-fuel combustion to surface $PM_{2.5}$. This approach assumes a linear response of surface $PM_{2.5}$ to changes in emissions.

Our choice of 2012 as the simulation year requires explanation. Air quality is influenced not just by emissions but also by meteorological variables such as surface temperature and wind speed, which can vary greatly on inter-annual timescales. Ideally, our analysis would involve multi-year simulations on both the coarse- and fine-scale grids, but such effort would be computationally expensive. We choose instead to do a one-year simulation for a year not influenced by El Niño conditions, which can worsen or ameliorate air pollution, depending on the region (e.g., Chang et al. (2016), Shen and Mickley (2017)). To gauge the error implied by our choice to simulate just one year rather than a span of years, we examine the inter-annual variation in total $PM_{2.5}$ concentrations at the surface estimated from the Dalhousie University archive (van Donkelaar et al., 2016). The $PM_{2.5}$ values in the Dalhousie archive are calculated by first combining satellite observations with GEOS-Chem estimates, and then calibrating the resulting concentrations with available ground-based observations (mostly Europe, the US, India and China). We find that the global mean average of the relative standard deviation of total $PM_{2.5}$ in the Dalhousie archive over 2008 to 2016 is just 7%. Averaged over large regions on the continental scale, the relative standard deviation ranges from 4% over Australia to 11% over the Asia nested grid domain (Figure S1). Inter-annual variability in this metric is greatest (> 60%) for smaller regions influenced by wildfires or biomass burning – e.g., Indonesia and remote areas at high northern latitudes where few people live. To test our choice of 2012 as a representative year,

we calculate the 2012 anomaly in the Dalhousie $PM_{2.5}$ time series (Figure S2). Again on a continental scale, we find that 2012 concentrations range from 0.7 μg m^{-3} less to 0.4 μg m^{-3} greater than the 2008-2016 average (Figure S2). Given the relatively small inter-annual variability in surface $PM_{2.5}$ in the Dalhousie archive over most populated regions, as well as the small anomalies in $PM_{2.5}$ in 2012 relative to the long-term mean, we conclude that the 2012 GEOS-Chem simulation provides a representative snapshot of global air quality.

To validate the 2012 $PM_{2.5}$ results from GEOS-Chem, we rely on archived $PM_{2.5}$ concentrations from the World Health Organization database (WHO). We find that GEOS-Chem captures the observed annual mean $PM_{2.5}$ concentrations with a correlation of 0.70, mean absolute error of 3.4 μg m^{-3}, and normalized mean bias of 27% (Figure S3). Our high bias in the US (where most North American WHO data are located) is opposite to the low bias estimated by Ford and Heald (2016) in urban (-25%) and rural (-6%) areas; such biases may be due to differences in US emission inventories for both gas-phase aerosol precursors and primary particles (Xing et al., 2015). A caveat in our comparison is that most observations (95%) in the WHO database with at least 75% temporal coverage in 2012 are in North America and Europe. We add to Figure S3 the 2012 observations from the US embassy in Shanghai (those for Beijing are already in the WHO dataset), and national monitoring sites embassies in Delhi (Cusworth et al., 2018), and the Highveld region in South Africa (South African Air Quality Information System; data obtained by request from the South African Weather Service in July 2018). Over the European domain in Figure S1, we find that GEOS-Chem yields a correlation of 0.60, mean absolute error of 5.2 μg m^{-3} and a normalized mean bias of 33% in surface $PM_{2.5}$; over the North American domain in Figure S1, these values are 0.52, 1.8 μg m^{-3} and 20% (Figure S4). Taken together, these validation statistics are similar to those reported by other studies examining surface $PM_{2.5}$ in global models (e.g., Shindell et al. (2018)) and regional models (e.g., Xing et al. (2015)) .

Table S1. GEOS-Chem anthropogenic emissions. All emissions are scaled to 2012 conditions.

Region	Inventory name	Species	Reference
Global	EDGAR v4.2[a,c]	NO, CO, SO_2, sulfate, ammonia	Olivier and Berdowski (2001)
Global	RETRO[a,c]	Non-methane VOCs	Schultz et al. (2007)
Global	---	Ethane	Xiao et al. (2008)
Global	GEIA	Biofuel ammonia	www.geiacenter.org
Global	BOND[a,c]	Carbonaceous particles	Bond et al. (2007)
Global	AEIC v2.0 aircraft	NO, CO, etc.	Stettler et al. (2011)
Global	ARTCAS ship	SO_2	Eyring et al. (2005)
Global	ICOADS ship	CO	C. Wang et al. (2008)
Global	PARANOX ship	NO	Vinken et al. (2011)
United States	NEI 2011[a,b,c]	Many species	US EPA, www3.epa.gov/airtrends
Europe	EMEP[b,c]	Many species	www.emep.int
Asia	MIX[c]	Many species	M. Li et al. (2017), Venkataraman et al. (2018), X. Li et al. (2018)
Africa	DICE[c,d]	Many species	Marais and Wiedinmyer (2016)
Africa	---	Open waste burning species	Wiedinmyer et al. (2014)

[a] Includes biofuel sources

[b] Includes ship emissions

[c] Includes land-based transport emissions

[d] Includes only diffuse and inefficient sources of anthropogenic emissions – residential fuelwood, diesel and petrol generators, ad-hoc oil refining, gas flares, kerosene use, charcoal production and use, road transport (including motorcycles). For emissions from formal industry and powerplants, we use the global inventories.

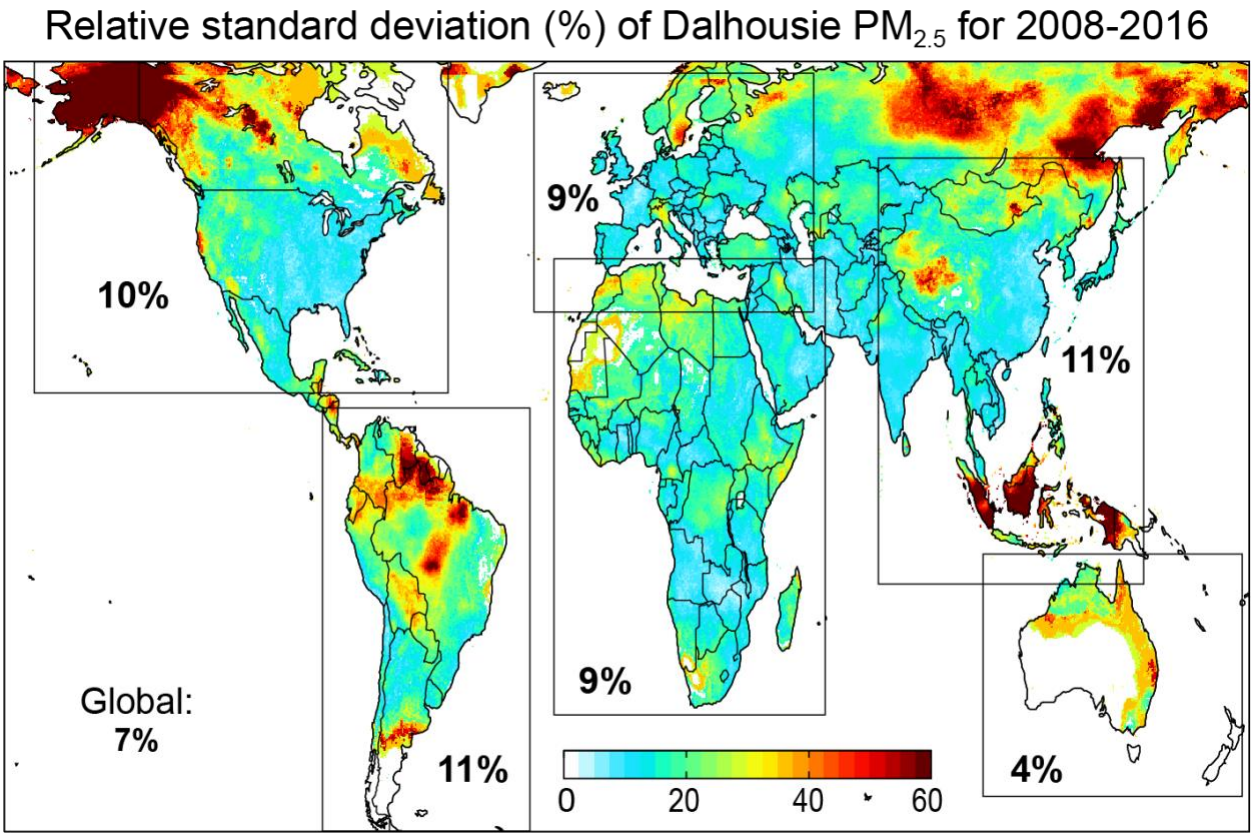

Figure S1. Uncertainty in 2012 $PM_{2.5}$ due to interannual variability. Interannual variability is estimated as the relative standard deviation of the Dalhousie satellite-derived $PM_{2.5}$ product (van Donkelaar et al., 2016) for 2008-2016 at 0.1°×0.1°. Values inset are the domain mean relative standard deviations for North America, South America, Western Europe (including portions of North Africa and the Middle East), Africa (including a portion of the Middle East), Southeast Asia, and Australia.

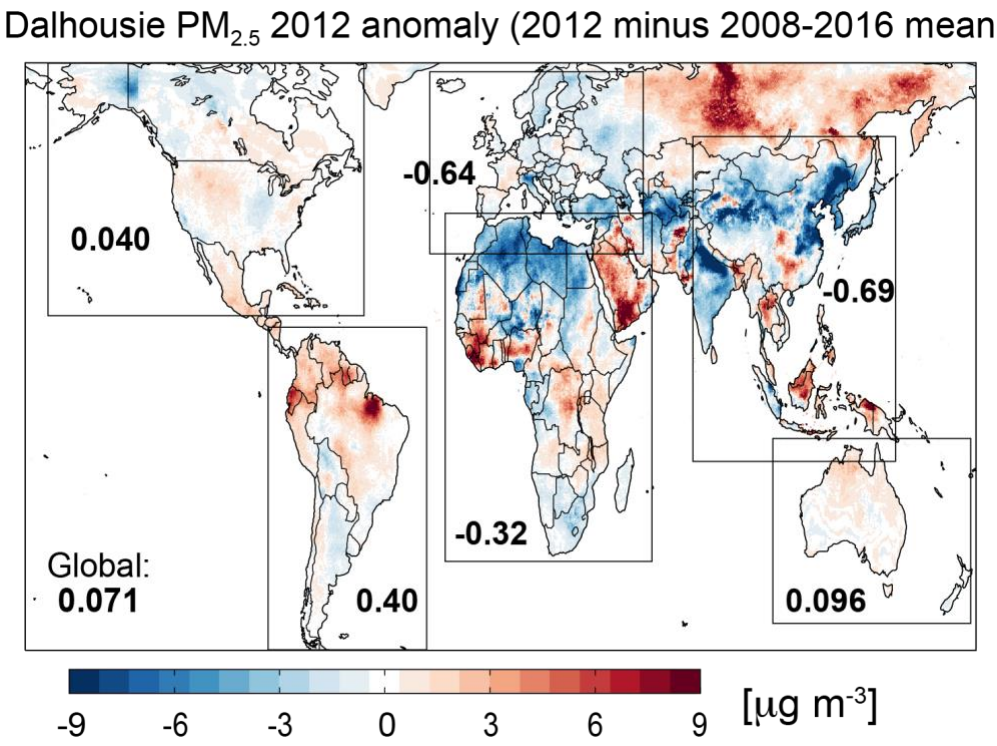

Figure S2. Representativeness of $PM_{2.5}$ in 2012, calculated as the absolute difference in 2012 and 2008-2016 mean $PM_{2.5}$ from Dalhousie (van Donkelaar et al., 2016) at 0.1°×0.1°. Values inset are domain mean anomalies for North America, South America, Western Europe (including portions of North Africa and the Middle East), Africa (including a portion of the Middle East), Southeast Asia, and Australia.

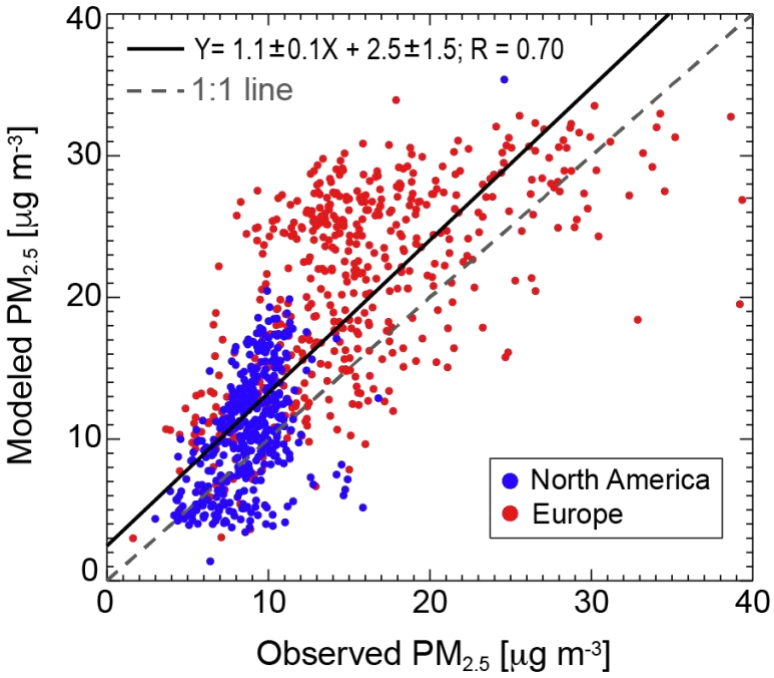

Figure S3. Evaluation of GEOS-Chem $PM_{2.5}$. Points are annual mean $PM_{2.5}$ for coincident 0.5°×0.667° grid squares with at least 75% temporal coverage in the observations. GEOS-Chem $PM_{2.5}$ is estimated at 50% relative humidity (RH) in Europe and 35% RH everywhere else, following standard protocols in measurements of $PM_{2.5}$. Reduced major axis (RMA) regression line (solid black line) and statistics, and the Pearson's correlation coefficient for all coincident grid squares are given inset. Points in red are in Europe and in blue are in North America. Only 7 out of 957 points exceed the range shown.

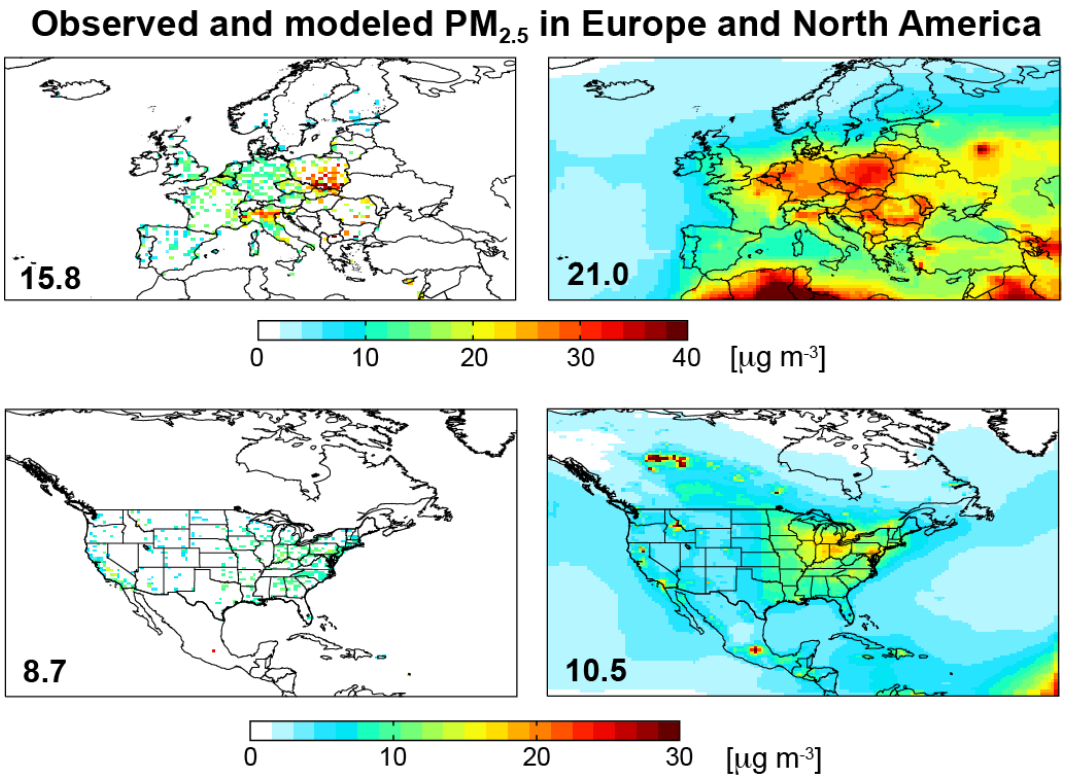

Figure S4. Comparison of the spatial distribution of observed and modeled $PM_{2.5}$ in Europe and North America. Data are on a uniform 0.5°×0.667° grid. Only observations with at least 75% temporal coverage are used. $PM_{2.5}$ are obtained at 50% RH in Europe and 35% RH in North America. Data for the two domains are plotted on different scales. Mean $PM_{2.5}$ for coincident grid squares is given inset

$PM_{2.5}$ mortality concentration –response model

We estimated the number of premature deaths attributable to fossil-fuel related $PM_{2.5}$ using a health impact function. To estimate the excess number of deaths associated with $PM_{2.5}$ exposure one requires estimates of exposure, the size of the population exposed, the mortality rate for that population, and the fraction of total deaths attributable to that exposure (AF%).

Recent meta-analysis of the association between long-term $PM_{2.5}$ and mortality (Vodonos et al., 2018) applied a multivariate linear random effects meta-analysis and meta-regression models that polled 135 hazard ratio estimates derived from 53 studies examined long-term $PM_{2.5}$ and mortality. This meta-analysis provided an evidence of a nonlinear association where the exposure-mortality slopes decreased at higher concentrations (**Figure S5)**. For example, each 1 μg m^{-3} increase in $PM_{2.5}$ was associated with a 1.29% increase in all-age all-cause mortality (95%CI 1.09-1.50) at a mean exposure of 10 μg m^{-3}, which decreased to 0.94 % (95%CI 0.76-1.12) at a mean exposure of 20 μg m^{-3}, to 0.81% (95%CI 0.52-1.12) at 30 μg m^{-3} and to 0.79% (95%CI 0.40-1.13) at 40 μg/$m^{3.}$

Hence, for examining a reduction of $PM_{2.5}$ levels from 15 to 10 μg/m^3, we calculated the mean slope as area under the curve between 0.014 and 0.011= 0.0125. A reduction of $PM_{2.5}$ levels from 30 to 20 μg/m^3, the mean slope was calculated as area under the curve between 0.009 and 0.008 = 0.00814

Mean value of estimates of mortality ($\bar{\beta}$) for each grid cell was calculated as area under the curve for the concentration-specific β in each grid cell from the low $PM_{2.5}$ scenario (without fossil fuel emissions) to the high $PM_{2.5}$ scenario (with all emissions, including fossil fuel) following the form shown in Equation

$$\bar{\beta}(PM_{2.5})=\int_{PM_{2.5}\ \text{no fossil fuel}}^{PM_{2.5}\ \text{all emissions}} \beta(PM_{2.5})$$

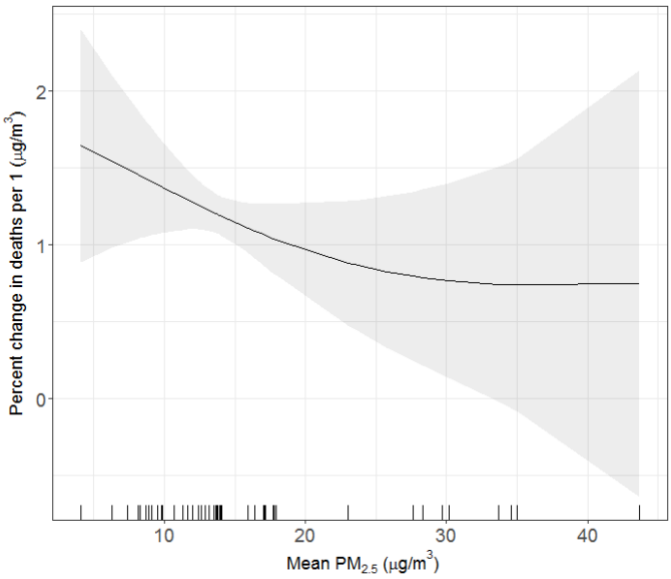

Figure S5. Estimates for long-term $PM_{2.5}$ mortality dose-response, drawn from the meta-analysis of long-term association between $PM_{2.5}$ and mortality (Vodonos et al., 2018).

Table S2. Extended data. Global regions, number of deaths, attributable fraction (%) for the population above 14 years old attributable to fine particulate matter ($PM_{2.5}$) exposure in 2012

Country name	Total Deaths >14 years old	Mean population weighted annual $PM_{2.5}$ ($\mu g\ m^{-3}$)			Attributable deaths[a]	Mean attributable fraction (%)[b]
		With all emission sources	Without fossil fuel	Estimated fossil fuel $PM_{2.5}$		
North America						
Bermuda	488	3	1.9	1.1	9	1.8
Greenland	472	1.2	0.9	0.3	3	0.6
Central America & the Caribbean						
Antigua and Barbuda	538	4.4	4.1	0.3	2	0.4
Bahamas	2,347	4.1	2.8	1.4	53	2.3
Barbados	2,523	4.9	4.7	0.2	7	0.3
Belize	1,530	5	4	1.1	26	1.7
Costa Rica	38,094	5.4	2.9	2.6	1,557	4.1
Cuba	95,635	5.3	3.8	1.5	2,334	2.4
Dominica	668	4.9	4.7	0.2	2	0.3
Dominican Republic	60,949	11.2	5.3	6	4,925	8.1
El Salvador	44,036	9.7	3.4	6.3	4,029	9.1
Grenada	983	4.6	4.3	0.4	6	0.6
Guatemala	67,426	9.7	3.2	6.5	6,205	9.2
Haiti	70,013	8.2	4.9	3.3	3,409	4.9
Honduras	40,564	7.9	3.5	4.4	2,620	6.5
Jamaica	18,511	9.1	4.7	4.4	1,183	6.4

Country name	Total Deaths >14 years old	Mean population weighted annual $PM_{2.5}$ ($\mu g\ m^{-3}$)			Attributable deaths[a]	Mean attributable fraction (%)[b]
		With all emission sources	Without fossil fuel	Estimated fossil fuel $PM_{2.5}$		
Mexico	615,874	11.8	2.4	9.5	65,871	10.7
Nicaragua	20,467	5.4	3.5	1.9	614	3.0
Panama	16,364	4.7	2.5	2.2	594	3.6
Puerto Rico	28,717	5.5	4.6	0.9	409	1.4
Saint Lucia	1,191	5	4.8	0.2	4	0.3
Saint Vincent and the Grenadines	913	4.7	4.5	0.2	3	0.3
Trinidad and Tobago	19,561	5.4	4.5	0.9	277	1.4
United States Virgin Islands	1,202	4.6	4.2	0.4	7	0.6
South America						
Argentina	306,979	7.9	3.4	4.5	20,385	6.6
Bolivia	50,854	5.7	4.4	1.3	1,095	2.2
Brazil	1,161,922	8.9	2.9	6.1	94,216	8.1
Chile	108,995	10	2.4	7.6	11,202	10.3
Colombia	247,981	8.2	2.7	5.5	20,045	8.1
Ecuador	74,588	6.7	2.1	4.6	5,357	7.2
Guyana	4,830	8	6.6	1.4	96	2.0
Paraguay	29,665	9.2	6	3.2	1,374	4.6
Peru	120,778	7.3	1.8	5.5	10,209	8.5
Suriname	3,667	6.9	6.2	0.7	36	1.0
Uruguay	30,980	6.5	2.4	4.1	1,967	6.3
Venezuela	247,407	10.6	4.3	6.2	21,185	8.6

Country name	Total Deaths >14 years old	Mean population weighted annual $PM_{2.5}$ ($\mu g\ m^{-3}$)			Attributable deaths[a]	Mean attributable fraction (%)[b]
		With all emission sources	Without fossil fuel	Estimated fossil fuel $PM_{2.5}$		
Europe						
Albania	20,072	19.8	8.6	11.2	2,458	12.2
Andorra	654	13.4	5.8	7.6	65	9.9
Austria	79,627	21.4	4.3	17.1	15,018	18.9
Belarus	115,131	20.6	2.9	17.8	23,397	20.3
Belgium	108,113	25.5	2.8	22.7	25,633	23.7
Bosnia and Herzegovina	36,427	21	6.8	14.2	5,628	15.5
Bulgaria	106,938	20.2	7.2	13	15,346	14.4
Croatia	52,156	20.2	5.6	14.6	8,454	16.2
Cyprus	7,171	15.4	9.2	6.3	543	7.6
Czech Republic	109,205	26.2	3.4	22.8	25,467	23.3
Denmark	51,600	16.3	2.1	14.2	9,202	17.8
Estonia	14,761	12.6	1.6	11	2,227	15.1
Finland	50,553	8.6	1.3	7.3	5,506	10.9
France	562,481	18.1	3.4	14.7	97,242	17.3
Georgia	51,550	23.3	10.2	13.1	6,670	12.9
Germany	896,319	23.9	3.2	20.7	198,569	22.2
Greece	116,757	15.6	8.1	7.5	10,616	9.1
Hungary	128,981	24.7	4.7	20	26,863	20.8
Iceland	1,891	2.6	1.6	1	31	1.6
Ireland	30,421	8.3	2	6.4	2,902	9.5
Italy	622,080	18.8	6	12.8	89,412	14.4
Kazakhstan	126,168	17.1	9.2	7.9	11,343	9.0

Country name	Total Deaths >14 years old	Mean population weighted annual $PM_{2.5}$ ($\mu g\ m^{-3}$)			Attributable deaths[a]	Mean attributable fraction (%)[b]
		With all emission sources	Without fossil fuel	Estimated fossil fuel $PM_{2.5}$		
Latvia	31,672	16.2	2	14.3	5,719	18.1
Lithuania	40,380	21.4	2.3	19.1	8,729	21.6
Malta	3,593	16	11.4	4.6	193	5.4
Moldova	43,245	25.4	5.2	20.2	8,922	20.6
Montenegro	6,223	18	7.9	10.1	724	11.6
Netherlands	143,387	24.2	2.7	21.5	32,972	23.0
Norway	29,299	5.9	1.4	4.5	2,065	7.0
Poland	393,724	26.5	3.1	23.4	93,842	23.8
Portugal	104,738	8.9	3.7	5.2	8,032	7.7
Romania	269,933	23.9	6.2	17.7	49,583	18.4
Russia	1,833,839	19	4.9	14.1	289,922	15.8
Serbia	100,172	24.8	6.9	17.9	18,076	18.0
Slovakia	53,258	24.9	4.1	20.8	11,522	21.6
Slovenia	19,680	21.7	5.3	16.3	3,528	17.9
Spain	418,063	12.9	4.8	8.1	44,603	10.7
Sweden	88,058	10	1.6	8.5	10,548	12.0
Switzerland	62,993	20.3	4.6	15.8	11,196	17.8
Turkey	361,723	18.2	8.1	10.1	41,811	11.6
Ukraine	731,672	19.4	5.1	14.3	120,217	16.4
United Kingdom	579,747	15.4	2	13.5	99,069	17.1

Country name	Total Deaths >14 years old	Mean population weighted annual $PM_{2.5}$ ($\mu g\ m^{-3}$)			Attributable deaths[a]	Mean attributable fraction (%)[b]
		With all emission sources	Without fossil fuel	Estimated fossil fuel $PM_{2.5}$		
Africa						
Algeria	142,304	31.4	20.5	10.9	13,295	9.3
Angola	100,845	15.4	14.1	1.3	1,537	1.5
Benin	42,616	40.4	36.2	4.2	1,450	3.4
Botswana	12,721	8.2	6	2.1	397	3.1
Burkina Faso	84,040	55.9	54.6	1.3	855	1.0
Burundi	44,973	16.2	15.4	0.8	419	0.9
Cameroon	118,759	39.7	38.2	1.5	1,520	1.3
Cape Verde	2,545	66.9	66	0.9	18	0.7
Central African Republic	41,111	30.7	30.1	0.6	178	0.4
Chad	56,523	59.8	58.7	1	460	0.8
Comoros	3,878	1.6	1.4	0.1	9	0.2
Congo	21,705	20.6	19.3	1.3	287	1.3
Cote d'Ivoire	111,211	29.3	28.2	1.1	1,065	1.0
Democratic Republic of the Congo	419,021	21.3	20.7	0.6	2,261	0.5
Djibouti	4,509	21.2	17.5	3.8	164	3.6
Egypt	392,226	56.7	40.2	16.5	46,783	11.9
Equatorial Guinea	4,679	10	9.5	0.5	32	0.7
Eritrea	20,386	31.3	28.5	2.8	444	2.2
Ethiopia	287,855	17	15.2	1.8	5,657	2.0
Gabon	13,783	11	10.5	0.5	90	0.7
Gambia	9,610	58	56	2	151	1.6

Country name	Total Deaths >14 years old	Mean population weighted annual $PM_{2.5}$ ($\mu g\ m^{-3}$)			Attributable deaths[a]	Mean attributable fraction (%)[b]
		With all emission sources	Without fossil fuel	Estimated fossil fuel $PM_{2.5}$		
Ghana	149,177	31.5	28.9	2.6	3,361	2.3
Guinea	63,691	49.7	48.8	1	467	0.7
Guinea-Bissau	9,223	51.9	50.6	1.3	89	1.0
Kenya	219,806	8.3	6.4	2	6,035	2.7
Lesotho	25,223	12.6	7.5	5.1	1,689	6.7
Liberia	19,482	25.3	24.7	0.7	113	0.6
Libya	26,745	42.3	34.3	8	1,565	5.9
Madagascar	97,088	3.7	3.3	0.4	641	0.7
Malawi	83,919	9.9	9.4	0.6	681	0.8
Mali	69,737	60.3	59.3	1	555	0.8
Mauritania	13,520	98.7	97.4	1.3	159	1.2
Mauritius	9,564	1.6	1.3	0.3	43	0.4
Morocco	186,609	23.8	16.9	6.9	12,436	6.7
Mozambique	163,474	6.8	6.3	0.5	1,309	0.8
Namibia	12,923	11.1	10.2	0.9	159	1.2
Niger	63,052	73.3	71.6	1.7	844	1.3
Nigeria	689,902	59.7	54.9	4.8	25,282	3.7
Rwanda	43,547	16.4	15.2	1.2	557	1.3
Sao Tome and Principe	821	5.5	5.4	0.1	2	0.2
Senegal	61,877	71.2	69.3	1.8	916	1.5
Seychelles	702	1.5	1.2	0.3	4	0.6
Sierra Leone	33,549	42	41	0.9	230	0.7
Somalia	47,288	9.5	8.3	1.3	789	1.7

Country name	Total Deaths >14 years old	Mean population weighted annual $PM_{2.5}$ ($\mu g\ m^{-3}$)			Attributable deaths[a]	Mean attributable fraction (%)[b]
		With all emission sources	Without fossil fuel	Estimated fossil fuel $PM_{2.5}$		
South Africa	487,500	21.9	11.7	10.2	45,134	9.3
Sudan[c]	165,624	35.3	33.6	1.7	2,197	1.3
Swaziland	9,954	10.6	6.7	3.9	534	5.4
Tanzania	202,713	6.9	6.4	0.5	1,660	0.8
Togo	34,797	36.6	34.4	2.1	617	1.8
Tunisia	59,521	25.5	17.1	8.3	4,711	7.9
Uganda	127,825	13.1	11.8	1.3	2,018	1.6
Zambia	71,697	12.7	12.2	0.6	511	0.7
Zimbabwe	88,229	10.5	9	1.6	1,797	2.0
Western Asia & the Middle East						
Afghanistan	148,817	20.9	13.9	7	11,153	7.5
Armenia	25,420	22.6	11.9	10.7	2,721	10.7
Azerbaijan	85,764	29.8	17.6	12.2	8,733	10.2
Bahrain	3,315	33.1	30.2	2.9	73	2.2
Iran	330,324	28.5	23.8	4.7	13,168	4.0
Iraq	95,874	30.1	26.4	3.7	2,942	3.1
Israel	40,291	21.2	14.4	6.9	2,776	6.9
Jordan	13,031	22.9	16.6	6.2	766	5.9
Kuwait	5,120	37.4	34.4	3	110	2.1
Kyrgyzstan	29,441	17.3	8.4	8.9	3,041	10.3
Lebanon	27,756	18	11.7	6.3	1,931	7.0
Oman	7,482	46.5	40.6	5.8	321	4.3

Country name	Total Deaths >14 years old	Mean population weighted annual $PM_{2.5}$ ($\mu g\ m^{-3}$)			Attributable deaths[a]	Mean attributable fraction (%)[b]
		With all emission sources	Without fossil fuel	Estimated fossil fuel $PM_{2.5}$		
Palestine	12,562	22.7	15.6	7.1	853	6.8
Qatar	4,252	35.2	31.7	3.5	109	2.6
Saudi Arabia	82,403	32.6	29.6	3	1,893	2.3
Syria	140,751	19.4	12.7	6.7	10,159	7.2
Tajikistan	38,948	21.7	9.6	12.1	4,914	12.6
Turkmenistan	51,096	31.7	26.4	5.3	2,124	4.2
United Arab Emirates	16,636	54	45.8	8.1	1,000	6.0
Uzbekistan	205,829	24.8	12.8	12	23,912	11.6
Yemen	90,616	23	19.9	3.1	2,520	2.8
Eastern Asia						
Bangladesh	692,081	58.9	6.7	52.3	252,927	36.5
Bhutan	2,909	23.6	5.7	17.9	516	17.7
Brunei	1,684	6.1	3.3	2.8	72	4.3
Cambodia	85,803	20.9	11.6	9.2	8,445	9.8
China	9,720,397	72.8	9.9	62.9	3,910,916	40.2
China (2018)[d]	9,720,397	41	9.7	31.2	2,355,579	24.2
India	8,009,357	52	9	42.9	2,458,384	30.7
Indonesia	1,495,066	20.9	5.7	15.3	230,097	15.4
Japan	1,284,769	22.6	4.6	18	242,561	18.9
Laos	33,822	19.6	8	11.6	4,404	13.0
Malaysia	154,090	18.9	5.3	13.6	22,228	14.4
Maldives	865	5.9	2.3	3.7	50	5.8

Country name	Total Deaths >14 years old	Mean population weighted annual $PM_{2.5}$ ($\mu g\ m^{-3}$)			Attributable deaths[a]	Mean attributable fraction (%)[b]
		With all emission sources	Without fossil fuel	Estimated fossil fuel $PM_{2.5}$		
Mongolia	12,013	8.4	4.8	3.5	628	5.2
Myanmar	340,623	16.4	7.4	9	36,978	10.9
Nepal	168,690	38.8	9.5	29.3	39,066	23.2
North Korea	201,841	35.8	5.3	30.5	52,942	26.2
Pakistan	1,115,784	36.7	15.1	21.7	188,406	16.9
Papua New Guinea	63,224	3.1	2.9	0.2	168	0.3
Philippines	559,792	8.7	2.1	6.7	51,203	9.1
Singapore	14,100	21.9	4.9	16.9	2,616	18.6
South Korea	265,641	44	5.3	38.8	80,962	30.5
Sri Lanka	116,032	13.4	3.5	9.9	14,998	12.9
Taiwan	164,488	14.5	3.2	11.3	23,711	14.4
Thailand	418,824	20.6	4.7	15.9	71,184	17.0
Timor-Leste	5,381	6.4	5	1.4	115	2.1
Vietnam	541,064	31.7	4.4	27.4	127,614	23.6
Australia & Oceania						
American Samoa	301	0.7	0.7	0	0	0.0
Australia	142,935	4.9	2.4	2.5	5,686	4.0
Federated States of Micronesia	679	0.7	0.7	0	1	0.1
Fiji	5,538	1.3	1.2	0.1	9	0.2
Guam	1,112	1.2	1	0.2	4	0.4
Kiribati	852	0.8	0.8	0	0	0.0
Marshall Islands	336	1.1	1.1	0	0	0.0

Country name	Total Deaths >14 years old	Mean population weighted annual $PM_{2.5}$ ($\mu g\ m^{-3}$)			Attributable deaths[a]	Mean attributable fraction (%)[b]
		With all emission sources	Without fossil fuel	Estimated fossil fuel $PM_{2.5}$		
New Zealand	29,923	2.2	1.5	0.6	320	1.1
Northern Mariana Islands	249	1.3	1.1	0.3	1	0.4
Samoa	960	0.7	0.7	0	0	0.0
Solomon Islands	3,286	1.2	1.2	0	2	0.1
Tonga	657	1.2	1.1	0.1	1	0.2
Vanuatu	1,791	2.2	2.2	0.1	2	0.1

USA						
State name	Total Deaths >14 years old	Mean population weighted annual $PM_{2.5}$ ($\mu g\ m^{-3}$)			Attributable deaths[a]	Mean attributable fraction (%)[b]
		With all emission sources	Without fossil fuel	Estimated fossil fuel $PM_{2.5}$		
Alabama	50,411	9.4	2.6	6.9	5,067	10.1
Alaska	3,384	2.2	1.4	0.9	51	1.5
Arizona	56,565	7.9	4	3.9	3,263	5.8
Arkansas	26,345	10.3	2.6	7.6	2,887	11.0
California	259,363	12.2	2.4	9.8	34,081	13.1
Colorado	36,885	6.8	3	3.8	2,140	5.8
Connecticut	32,639	12.1	1.7	10.5	4,749	14.6
Delaware	4,436	13.2	1.7	11.5	694	15.6
Florida	191,646	6.6	2.4	4.2	12,483	6.5
Georgia	75,518	11.3	2.5	8.8	9,290	12.3

State name	Total Deaths >14 years old	Mean population weighted annual $PM_{2.5}$ ($\mu g\ m^{-3}$)			Attributable deaths[a]	Mean attributable fraction (%)[b]
		With all emission sources	Without fossil fuel	Estimated fossil fuel $PM_{2.5}$		
Hawaii	11,032	2.6	2.1	0.4	83	0.8
Idaho	13,006	6.2	3.3	2.8	581	4.5
Illinois	102,593	16.6	1.9	14.7	18,952	18.5
Indiana	66,979	17	1.9	15.1	12,637	18.9
Iowa	33,378	11.9	2.1	9.8	4,562	13.7
Kansas	33,671	10.4	1.9	8.5	4,094	12.2
Kentucky	52,325	14.3	2	12.4	8,500	16.2
Louisiana	42,176	10.4	2.8	7.5	4,505	10.7
Maine	14,555	7.7	1.6	6.1	1,350	9.3
Maryland	40,784	15.8	1.8	14.1	7,336	18.0
Massachusetts	53,851	11.8	1.6	10.2	7,654	14.2
Michigan	93,585	16.7	1.8	14.9	17,438	18.6
Minnesota	39,674	13.3	2.2	11.1	5,877	14.8
Mississippi	40,360	10	2.6	7.3	4,263	10.6
Missouri	48,205	11.2	2.1	9.1	6,161	12.8
Montana	9,520	5.1	3.4	1.7	266	2.8
Nebraska	13,881	9	2.1	7	1,432	10.3
Nevada	23,541	6.7	3.4	3.3	1,192	5.1
New Hampshire	12,314	10	1.6	8.3	1,495	12.1
New Jersey	97,747	15.7	1.6	14.1	17,646	18.1
New Mexico	21,308	4.9	2.2	2.7	938	4.4
New York	129,489	14.6	1.6	13	21,931	16.9
North Carolina	95,239	12.5	2.2	10.3	13,357	14.0

State name	Total Deaths >14 years old	Mean population weighted annual $PM_{2.5}$ ($\mu g\ m^{-3}$)			Attributable deaths[a]	Mean attributable fraction (%)[b]
		With all emission sources	Without fossil fuel	Estimated fossil fuel $PM_{2.5}$		
North Dakota	4,070	6.9	2	4.9	309	7.6
Ohio	115,955	16.8	1.7	15	21,818	18.8
Oklahoma	40,908	8.7	1.9	6.8	4,190	10.2
Oregon	38,128	8.1	2.4	5.6	3,152	8.3
Pennsylvania	133,771	17.1	1.7	15.4	25,382	19.0
Rhode Island	4,910	10	1.6	8.3	597	12.2
South Carolina	51,014	10.9	2.5	8.4	6,048	11.9
South Dakota	7,036	7.4	2.1	5.4	574	8.2
Tennessee	67,804	11.4	2.1	9.3	8,844	13.0
Texas	183,885	8.4	1.9	6.4	17,663	9.6
Utah	16,534	6.5	2.7	3.8	981	5.9
Vermont	6,415	9.8	1.6	8.2	770	12.0
Virginia	71,555	13.9	2	11.9	11,206	15.7
Washington	50,955	7.7	2.3	5.4	4,138	8.1
West Virginia	22,500	11	1.9	9.1	2,900	12.9
Wisconsin	59,470	14.7	2	12.7	9,842	16.5
Wyoming	3,642	4.7	2.8	1.9	114	3.1

Canada						
Province name	Total Deaths >14 years old	Mean population weighted annual $PM_{2.5}$ ($\mu g\ m^{-3}$)			Attributable deaths[a]	Mean attributable fraction (%)[b]
		With all emission sources	Without fossil fuel	Estimated fossil fuel $PM_{2.5}$		
Alberta	21,535	8	2	6	1,958	9.1
British Columbia	33,403	8.7	1.9	6.8	3,237	9.7
Manitoba	9,868	7.9	2.7	5.2	778	7.9
New Brunswick	7,095	4.8	1.5	3.4	391	5.5
Newfoundland & Labrador	1,588	2.4	1.4	1	27	1.7
Northwest Territories	172	3.2	2.8	0.4	1	0.6
Nova Scotia	9,158	4.9	1.6	3.3	497	5.4
Nunavut	129	1.2	0.8	0.4	1	0.8
Ontario	90,996	15	1.6	13.4	15,728	17.3
Prince Edward Island	1,269	4.3	1.4	2.9	61	4.8
Quebec	66,494	13.9	1.6	12.3	10,645	16.0
Saskatchewan	8,515	7.5	2.4	5.2	678	8.0
Yukon Territory	193	1.1	0.9	0.3	1	0.5

[a] Annual number of deaths attributed to long term exposure to $PM_{2.5}$ generated by fossil fuel combustion.

[b] Mean proportion of deaths attributed to long term exposure to fossil-fuel related $PM_{2.5}$.

[c] Includes South Sudan

[d] Estimates derived after applying a 43.7% reduction to $PM_{2.5}$ from all sources for China

References

1. Aunan, K., Ma, Q., Lund, M. T., et al., Population-weighted exposure to $PM_{2.5}$ pollution in China: An integrated approach, Environ Int, 120, 111-120, doi:10.1016/j.envint.2018.07.042, 2018.

2. Bond, T. C., Bhardwaj, E., Dong, R., et al., Historical emissions of black and organic carbon aerosol from energy-related combustion, 1850-2000, Global Biogeochem Cy, 21, doi:10.1029/2006gb002840, 2007.

3. Burnett, R., Chen, H., Szyszkowicz, M., et al., Global estimates of mortality associated with long-term exposure to outdoor fine particulate matter, P Natl Acad Sci USA, 115, 9592-9597, doi:10.1073/pnas.1803222115, 2018.

4. Chang, L. Y., Xu, J. M., Tie, X. X., et al., Impact of the 2015 El Nino event on winter air quality in China, Sci Rep-Uk, 6, doi:10.1038/srep34275, 2016.

5. Cusworth, D. H., Mickley, L. J., Sulprizio, M. P., et al., Quantifying the influence of agricultural fires in northwest India on urban air pollution in Delhi, India, Environ Res Lett, 13, doi:10.1088/1748-9326/aab303, 2018.

6. Di, Q., Koutrakis, P., Schwartz, J., A hybrid prediction model for $PM_{2.5}$ mass and components using a chemical transport model and land use regression, Atmos Environ, 131, 390-399, doi:10.1016/j.atmosenv.2016.02.002, 2016.

7. Eyring, V., Kohler, H. W., van Aardenne, J., et al., Emissions from international shipping: 1. The last 50 years, J Geophys Res-Atmos, 110, doi:10.1029/2004jd005619, 2005.

8. Fairlie, T. D., Jacob, D. J., Park, R. J., The impact of transpacific transport of mineral dust in the United States, Atmos Environ, 41, 1251-1266, doi:10.1016/j.atmosenv.2006.09.048, 2007.

9. Ford, B., Heald, C. L., Exploring the uncertainty associated with satellite-based estimates of premature mortality due to exposure to fine particulate matter, Atmos Chem Phys, 16, 3499-3523, doi:10.5194/acp-16-3499-2016, 2016.

10. Fountoukis, C., Nenes, A., ISORROPIA II: a computationally efficient thermodynamic equilibrium model for K^+-Ca^{2+}-Mg^{2+}-Nh_4^+-Na^+-SO_4^{2-}-NO_3^--Cl^--H_2O aerosols, Atmos Chem Phys, 7, 4639-4659, doi:10.5194/acp-7-4639-2007, 2007.

11. Giglio, L., Randerson, J. T., van der Werf, G. R., Analysis of daily, monthly, and annual burned area using the fourth-generation global fire emissions database (GFED4), J Geophys Res-Biogeo, 118, 317-328, doi:10.1002/jgrg.20042, 2013.

12. Guenther, A. B., Jiang, X., Heald, C. L., et al., The Model of Emissions of Gases and Aerosols from Nature version 2.1 (MEGAN2.1): an extended and updated framework for modeling biogenic emissions, Geosci Model Dev, 5, 1471-1492, doi:10.5194/gmd-5-1471-2012, 2012.

13. Heald, C. L., Coe, H., Jimenez, J. L., et al., Exploring the vertical profile of atmospheric organic aerosol: comparing 17 aircraft field campaigns with a global model, Atmos Chem Phys, 11, 12673-12696, doi:10.5194/acp-11-12673-2011, 2011.

14. Heald, C. L., Jacob, D. J., Turquety, S., et al., Concentrations and sources of organic carbon aerosols in the free troposphere over North America, J Geophys Res-Atmos, 111, doi:10.1029/2006jd007705, 2006.

15. Hudman, R. C., Moore, N. E., Mebust, A. K., et al., Steps towards a mechanistic model of global soil nitric oxide emissions: implementation and space based-constraints, Atmos Chem Phys, 12, 7779-7795, doi:10.5194/acp-12-7779-2012, 2012.

16. Jaegle, L., Quinn, P. K., Bates, T. S., et al., Global distribution of sea salt aerosols: new constraints from in situ and remote sensing observations, Atmos Chem Phys, 11, 3137-3157, doi:10.5194/acp-11-3137-2011, 2011.

17. Keller, C. A., Long, M. S., Yantosca, R. M., et al., HEMCO v1.0: a versatile, ESMF-compliant component for calculating emissions in atmospheric models, Geosci Model Dev, 7, 1409-1417, doi:10.5194/gmd-7-1409-2014, 2014.

18. Lee, H. M., Park, R. J., Henze, D. K., et al., $PM_{2.5}$ source attribution for Seoul in May from 2009 to 2013 using GEOS-Chem and its adjoint model, Environ Pollut, 221, 377-384, doi:10.1016/j.envpol.2016.11.088, 2017.

19. Li, M., Zhang, Q., Kurokawa, J., et al., MIX: a mosaic Asian anthropogenic emission inventory under the international collaboration framework of the MICS-Asia and HTAP, Atmos Chem Phys, 17, 935-963, doi:10.5194/acp-17-935-2017, 2017.

20. Li, X., Wu, J. R., Elser, M., et al., Contributions of residential coal combustion to the air quality in Beijing-Tianjin-Hebei (BTH), China: a case study, Atmos Chem Phys, 18, 10675-10691, doi:10.5194/acp-18-10675-2018, 2018.

21. Li, Y., Henze, D. K., Jack, D., et al., The influence of air quality model resolution on health impact assessment for fine particulate matter and its components, Air Qual Atmos Health, 9, 51-68, doi:10.1007/s11869-015-0321-z, 2016.

22. Liu, H. Y., Jacob, D. J., Bey, I., et al., Constraints from ^{210}Pb and ^{7}Be on wet deposition and transport in a global three-dimensional chemical tracer model driven by assimilated meteorological fields, J Geophys Res-Atmos, 106, 12109-12128, doi:10.1029/2000jd900839, 2001.

23. Mao, J. Q., Paulot, F., Jacob, D. J., et al., Ozone and organic nitrates over the eastern United States: Sensitivity to isoprene chemistry, J Geophys Res-Atmos, 118, 11256-11268, doi:10.1002/jgrd.50817, 2013.

24. Marais, E. A., Jacob, D. J., Turner, J. R., et al., Evidence of 1991-2013 decrease of biogenic secondary organic aerosol in response to SO_2 emission controls, Environ Res Lett, 12, doi:10.1088/1748-9326/aa69c8, 2017.

25. Marais, E. A., Wiedinmyer, C., Air Quality Impact of Diffuse and Inefficient Combustion Emissions in Africa (DICE-Africa), Environ Sci Technol, 50, 10739-10745, doi:10.1021/acs.est.6b02602, 2016.

26. Murray, L. T., Jacob, D. J., Logan, J. A., et al., Optimized regional and interannual variability of lightning in a global chemical transport model constrained by LIS/OTD satellite data, J Geophys Res-Atmos, 117, doi:10.1029/2012jd017934, 2012.

27. Olivier, J. G. J., Berdowski, J. J. M., Global emission sources and sinks. The Climate System. A.A. Balkema Publishers/Swets & Zeitlinger Publishers, Lisse, The Netherlands, 2001, pp. 33-78.

28. Park, R. J., Jacob, D. J., Field, B. D., et al., Natural and transboundary pollution influences on sulfate-nitrate-ammonium aerosols in the United States: Implications for policy, J Geophys Res-Atmos, 109, doi:10.1029/2003jd004473, 2004.

29. Pye, H. O. T., Liao, H., Wu, S., et al., Effect of changes in climate and emissions on future sulfate-nitrate-ammonium aerosol levels in the United States, J Geophys Res-Atmos, 114, doi:10.1029/2008jd010701, 2009.

30. Schultz, M. G., Backman, L., Balkanski, Y., et al., REanalysis of the TROpospheric chemical composition over the past 40 years: Final report. http://hdl.handle.net/11858/00-001M-0000-0011-FBDD-B, 2007.

31. Shen, L., Mickley, L. J., Effects of El Nino on Summertime Ozone Air Quality in the Eastern United States, Geophys Res Lett, 44, 12543-12550, doi:10.1002/2017gl076150, 2017.

32. Shindell, D., Faluvegi, G., Seltzer, K., et al., Quantified, localized health benefits of accelerated carbon dioxide emissions reductions, Nat Clim Change, 8, doi:10.1038/s41558-018-0108-y, 2018.

33. Silvern, R. F., Jacob, D. J., Kim, P. S., et al., Inconsistency of ammonium-sulfate aerosol ratios with thermodynamic models in the eastern US: a possible role of organic aerosol, Atmos Chem Phys, 17, 5107-5118, doi:10.5194/acp-17-5107-2017, 2017.

34. Stettler, M. E. J., Eastham, S., Barrett, S. R. H., Air quality and public health impacts of UK airports. Part I: Emissions, Atmos Environ, 45, 5415-5424, doi:10.1016/j.atmosenv.2011.07.012, 2011.

35. Travis, K. R., Jacob, D. J., Fisher, J. A., et al., Why do models overestimate surface ozone in the Southeast United States?, Atmos Chem Phys, 16, 13561-13577, doi:10.5194/acp-16-13561-2016, 2016.

36. van Donkelaar, A., Martin, R. V., Brauer, M., et al., Global Estimates of Fine Particulate Matter using a Combined Geophysical-Statistical Method with Information from Satellites, Models, and Monitors, Environ Sci Technol, 50, 3762-3772, doi:10.1021/acs.est.5b05833, 2016.

37. van Donkelaar, A., Martin, R. V., Leaitch, W. R., et al., Analysis of aircraft and satellite measurements from the Intercontinental Chemical Transport Experiment (INTEX-B) to quantify long-range transport of East Asian sulfur to Canada, Atmos Chem Phys, 8, 2999-3014, doi:10.5194/acp-8-2999-2008, 2008.

38. Venkataraman, C., Brauer, M., Tibrewal, K., et al., Source influence on emission pathways and ambient $PM_{2.5}$ pollution over India (2015-2050), Atmos Chem Phys, 18, 8017-8039, doi:10.5194/acp-18-8017-2018, 2018.

39. Vinken, G. C. M., Boersma, K. F., Jacob, D. J., et al., Accounting for non-linear chemistry of ship plumes in the GEOS-Chem global chemistry transport model, Atmos Chem Phys, 11, 11707-11722, doi:10.5194/acp-11-11707-2011, 2011.

40. Vodonos, A., Abu Awad, Y., Schwartz, J., The concentration-response between long-term $PM_{2.5}$ exposure and mortality; A meta-regression approach, Environ Res, 166, 677-689, doi:10.1016/j.envres.2018.06.021, 2018.

41. Wang, C., Corbett, J. J., Firestone, J., Improving spatial representation of global ship emissions inventories, Environ Sci Technol, 42, 193-199, doi:10.1021/es0700799, 2008.

42. Wang, Q. Q., Jacob, D. J., Spackman, J. R., et al., Global budget and radiative forcing of black carbon aerosol: Constraints from pole-to-pole (HIPPO) observations across the Pacific, J Geophys Res-Atmos, 119, 195-206, doi:10.1002/2013jd020824, 2014.

43. Wang, S. W., Zhang, Q., Streets, D. G., et al., Growth in NO_x emissions from power plants in China: bottom-up estimates and satellite observations, Atmos Chem Phys, 12, 4429-4447, doi:10.5194/acp-12-4429-2012, 2012.

44. WHO, Ambient and household air pollution and health. World Health Organization, http://www.who.int/airpollution/data/en/.

45. Wiedinmyer, C., Yokelson, R. J., Gullett, B. K., Global Emissions of Trace Gases, Particulate Matter, and Hazardous Air Pollutants from Open Burning of Domestic Waste, Environ Sci Technol, 48, 9523-9530, doi:10.1021/es502250z, 2014.

46. Xiao, Y. P., Logan, J. A., Jacob, D. J., et al., Global budget of ethane and regional constraints on US sources, J Geophys Res-Atmos, 113, doi:10.1029/2007jd009415, 2008.

47. Xing, J., Mathur, R., Pleim, J., et al., Can a coupled meteorology-chemistry model reproduce the historical trend in aerosol direct radiative effects over the Northern Hemisphere?, Atmos Chem Phys, 15, 9997-10018, doi:10.5194/acp-15-9997-2015, 2015.

48. Zender, C. S., Bian, H. S., Newman, D., Mineral Dust Entrainment and Deposition (DEAD) model: Description and 1990s dust climatology, J Geophys Res-Atmos, 108, doi:10.1029/2002jd002775, 2003.

49. Zhang, L., Jacob, D. J., Knipping, E. M., et al., Nitrogen deposition to the United States: distribution, sources, and processes, Atmos Chem Phys, 12, 4539-4554, doi:10.5194/acp-12-4539-2012, 2012.

50. Zhang, L. M., Gong, S. L., Padro, J., et al., A size-segregated particle dry deposition scheme for an atmospheric aerosol module, Atmos Environ, 35, 549-560, doi:10.1016/S1352-2310(00)00326-5, 2001.